DESIGN LIMIT ANALYSIS OF
REDUNDANT TUBE ARRAY FIRST WALLS

P.J. Gierszewski

B.Mikic

N.E. Todreas

December 1982

Massachusetts Institute of Technology

Cambridge, MA 02139

Design Limit Analysis of Redundant Tube Array First Walls

P.J. Gierszewski

B.Mikic

N.E. Todreas

Abstract

Many fusion reactor designs use arrays of cooling tubes or simple variations of this proven heat transfer technolocy for the first wall. However, no complete solution exists for handling the inevitable leaks that will develop in this complex and critical tube array structure. Here we consider an approach that designs for leaks – that is, it permits a reasonable level of leak-tolerance in the design. In particular, each tube is designed with sufficient operating margin to handle the extra load if adjacent tubes are turned off because of leaks. This redundancy requirement is examined using a design window analysis, where it is treated as just another one of many constraints. The results indicate that leak-tolerance is possible under reasonable power reactor conditions.

Design Limit Analysis of Redundant Tube Array First Walls

P.J.Gierszewski, B.Mikic and N.Todreas

1.0 Introduction

Many fusion reactor first wall designs use an array of cooling tubes [1,2,3,4,5] or simple variations such as milled holes in armored blocks or corrugated channels [24]. This method provides good heat transfer ability in the critical plasma-wall interface region where radiated power and undiverted particles are intercepted.

Since there will be several thousand of these tubes operating in a high heat flux, high neutron flux, high erosion rate environment with internal pressurization and possible exotic structural materials and coolants, the probability of a leak is appreciable. Unfortunately, even a small leak into the near-vacuum of the plasma chamber can shut the reactor down. This leads to very tough requirements for the tubes.

The state-of-the-art in large-scale tube-array structures for heat transfer is exemplified by fission reactor steam generators and fuel pins. These operate in a high heat flux (0.1 kW/cm^2), high radiation flux (in the case of fuel pins) environment with internal pressurization (primary loop coolant or fill gas) and fairly conventional materials (steel, zirconium, water). Furthermore, they are manufactured to meet tight quality constraints. However, their performance does not meet the requirements for a fusion reactor first wall. Many steam generators, originally intended to last 30 years, are having tubes blocked or retubed, or are even being entirely replaced because of leaks. They are a major maintenance item [29]. The fuel pins, intended to operate for 1 to 3 years, fare much better. Nonetheless, there are enough defects in the fuel pin cladding at the end of each year to release appreciable amounts of fission products into the primary coolant loop [34].

Given this background, how well can we expect tube arrays to perform in the harsher but yet more leak-sensitive environment of a fusion reactor first wall? Generally, reactor designs try to reduce the load on the first wall (e.g. with divertors), design the first wall for a conservatively short life, and/or design the first wall for easy replacement in the event of a leak. While all these approaches are probably needed, they may not be sufficient. Uncertainties in the actual efficiency of divertors are large, and the cost penalties because of downtime are high for the short life/easy replacement scenarios. What is really needed

is redundancy and the ability to run the first wall with the inevitable leaks, at least until the next scheduled maintenance period. As an example, we suggest here a simple approach that provides some measure of the desired redundancy or leak-tolerant philosophy and design _for_ leaks, rather than trying to completely avoid them:

Consider alternate first wall tubes connected onto different headers. Suppose, then, that some isolated tubes fail – either they become blocked or start leaking. In such events, it is assumed that the faulty tubes can be identified, emptied of coolant and sealed, but otherwise left in place (much as is done in steam generators now). Ideally, each first wall tube could be sealed separately by a simple valve. In practice, each first wall would probably have two or three headers that could be remotely shut off, losing cooling to their respective tubes. The result is the elimination of coolant leakage into the plasma from, and pressure stresses on, the failed tube. The sole remaining constraint is to keep the failed tube peak temperature below melting, as well as any other affected tubes. If the tubes are connected such that immediate neighbour tubes are not also shut down, then the heat deposited in the failed tube can be conducted away.

In this report, we examine this redundant tube array approach using a design window analysis. That is, rather than performing a detailed heat transfer analysis, we consider the redundancy requirement as just another constraint out of many (possibly conflicting) constraints for a fusion reactor first wall. Then we can determine if this leak-tolerant approach poses an unreasonable constraint within the overall context. The design window approach has been used to a limited extent already for tube arrays [6,7,30], but here we allow for a wider range of coolant-material combinations and include redundancy in the design.

In Section 2, the constraints and physical models are explained; in Section 3, the materials properties and limits are given; and in Sections 4 and 5, the results are analyzed.

2.0 Physical Models

A general toroidal geometry with a circular cross-section is assumed. The tubes are taken to be straight, although curvature effects may be important if the tube length is a large fraction of the machine radius. No attempt is made to analyze the header and valving arrangements. In the present model, four broad "limit" categories are treated:

temperature, stress, incident flux and maintenance. On the basis of these constraints, mathematical equations are derived to relate basic variables to the limits.

2.1 Energy Removal

The coolant velocity u is fixed by requiring that the heat input be removed with a temperature rise ΔT_c along length x.

From an energy balance,

$$\pi R^2 u \rho_c c_r \Delta T_c = [2(f_r + f_p)Rq'' + 2\pi R q_s'''t + .\pi R^2 q_c''']xM \tag{1}$$

where ρ and c are the density and specific heat capacity; subscripts c and s refer to coolant and structure respectively; q'' is the total neutron energy flux at the first wall; q''' is the volumetric heat generation rate; f_p and f_r are the particle and radiation energy fluxes as fractions of the neutron flux; R is the tube radius; t is the tube thickness; and M is a multiplying factor to include additional heat input from failed adjacent tubes.

Solving for velocity and expressing it as a Reynolds number,

$$Re = [2(f_r + f_p) + 2\pi \Sigma_s t + \pi R \Sigma_c]\frac{2q''xM}{\mu_c c_c \Delta T_c} \tag{2}$$

where $q''' = q''\Sigma$ and Σ is the macroscopic neutron interaction cross-section. Thus, velocity (and thus flow rate) is an internal variable in this design window analysis. It is kept within bounds via constraints on pressure drop discussed later.

A general form for the heat transfer coefficient h is used to accommodate a variety of coolants,

$$Nu = \frac{2Rh}{k_c} = h_0 + h_1 Re^{h_2} \tag{3}$$

where Nu is the Nusselt number and k_c is coolant thermal conductivity. In particular, for helium, water and flibe ($Pr = \mu_c c_c/k_c > 0.5$) [8],

$$Nu = \frac{2Rh}{k_c} = 0.023 Pr^{0.4} Re^{0.8} \tag{4}$$

and for lithium and sodium ($Pr < 0.05$) [8],

$$Nu = 6.7 + 0.025(RePr)^{0.8} \tag{5a}$$

in the absence of a magnetic field, and [36]

$$Nu = 7 \tag{5b}$$

in a typical tokamak (the fields reduce heat transfer by inhibiting turbulence).

The heat flux is assumed to be uniform around the tube in order to calculate temperature differences across the tube and film. The accuracy of this depends on the particle and radiation flux compared to the volumetric neutron heating rate and the conductivity of the tube material.

2.2 Temperature Limits

The hottest point along each tube is at the exit, assuming a uniform energy flux. At this point, the tube inner surface cannot exceed a corrosion or chemical compatibility temperature limit T_c,

$$T_{in} + \Delta T_c + \frac{q''}{h}\left[\frac{f_r + f_p}{\pi} + \Sigma_s t\right] \leq T_c \qquad (6)$$

where the last term is the film temperature rise, ΔT_{film}. Note that contributions from the plasma (radiation and particles), and neutron interactions in the first wall structure are included, but nuclear heating of the first wall coolant is neglected.

Appreciable degradation in mechanical properties occurs at a sufficiently high temperature T_m, which poses an upper bound on the hottest point in the tube itself,

$$T_{in} + \Delta T_c + \Delta T_{film} + q''\left[\frac{(f_r + f_p)t}{k_s} + \frac{\Sigma_s t^2}{2k_s}\right] \leq T_m \qquad (7)$$

where the fourth term is the temperature rise across the heated tube wall, ΔT_{wall}.

The final temperature limit is based on the redundancy criterion. Considering the first wall area and the harsh environment, tubes are likely to suffer from the development of small cracks which, while structurally small, may leak enough coolant into the plasma to quench it. It is highly desirable for continued operation even with a small number of isolated tubes not working – they may be blocked or have a leak. In such events, it is assumed that the faulty tubes are identified, emptied of coolant and sealed, but otherwise left in place. This eliminates coolant leakage into the plasma and pressure stresses on the tube. The constraint is then to keep the failed tube peak temperature below melting. If tubes are connected such that immediate neighbour tubes are not also shut down, then the heat deposited in the failed tube can be conducted to these. Simplifying the problem to a 1-D slab under a uniform heat flux [9],

$$T_{in} + \Delta T_c + \Delta T_{film} + \Delta T_{wall} + \frac{q''R^2}{k_s}\left[\frac{\pi^2 \Sigma_s}{8} + \frac{f_r + f_p}{t}\right] \leq T_l \qquad (8)$$

5

where T_l is the leak temperature limit (i.e. the melting point) and the term in brackets is the temperature rise from the failed tube's plasma side to its contact point with the nearest neighbour, itself limited to T_m at the contact point. This implies alternating tubes on separate headers, with all tubes on a particular header shut down by a header valve when any one develops a leak. If every second tube is on the same header, than the unfailed tubes must be able to handle 100% more energy until the next downtime ($M = 2.0$ in Eqn.1). If every third or more tube is on the same header, then $M = 1.5$.

Note that the corrosion and mechanical temperature limits, Eqns.(6) and (7), are for normal operation ($M = 1$ assumed). If adjacent tubes have failed, these limits may be locally exceeded, but it is assumed that the increase will be tolerable until the next maintenance period when the first wall module containing these plus the failed tubes is replaced.

2.3 Stress Limits

The hoop stress caused by coolant pressure is a primary membrane stress and is limited to

$$\frac{pR}{t} \leq S_{mt} \tag{9}$$

where S_{mt} is the maximum allowable primary membrane stress; and p is the coolant pressure.

Thermal stresses and other secondary membrane stress components are not treated. However, thermal stresses produce a peak stress which determines fatigue life, based on the non-uniform thermal expansion and contraction of the tubes during the burn cycle. Through-thickness, axial and azimuthal temperature differences all contribute. While the exact stress depends on the nature of the header/tube interface (a region not included in the present analysis, but treated in more detail in Ref.[35]), the through-thickness thermal strain ($\Delta \epsilon$) is a major contributor to fatigue life reduction [10] and can be estimated as

$$\frac{\alpha_s q''}{k_s(1 - \nu_s)} \left[\frac{\Sigma_s t^2}{3} + \frac{t(f_r + f_p)}{2} \right] \leq \Delta \epsilon_{max} \tag{10}$$

where α_s is the coefficient of thermal expansion and ν_s is Poisson's ratio. Also, while proper design of the tubes can reduce axial strain by allowing free expansion (or by higher coolant flow rate), and reduce azimuthal strain with high thermal conductivity layers to spread out the surface heat load, the through-thickness term will always be present.

6

The maximum allowable strain range comes from fitted curves relating $\Delta\epsilon_{max}$ to the total number of cycles.

The pressure drop Δp in the tubes themselves is generally small and not included in the stress calculations. It does contribute to the overall pumping power requirements and there is a limit based on the ratio of pumping power to the thermal energy picked up by the tubes. For electrically conducting fluids, the tubes are assumed to be parallel to the field so MHD pressure losses are neglected. Consequently only friction contributes to the pumping power limit P^* in the first wall tubes

$$\frac{\Delta p}{\rho_c c_c \Delta T_c} \leq P^* \tag{11}$$

where

$$\Delta p = \phi\left(\frac{x}{2R}\right)\left(\frac{\rho_c u^2}{2}\right) \tag{12}$$

and the friction factor ϕ can be expressed by standard correlations of the form

$$\phi = \phi_1/Re^{\phi_2} \tag{13}$$

Pressure drops in the headers may be more important, but cannot be considered unless more specific header and connecting line arrangements are assumed [11]. We avoid detailed hardware specifications here, and the penalty is that this constraint is "soft".

2.4 Incident Flux Limits

The incident flux is composed of neutrons, particles and radiation. The fusion energy is mostly in the neutrons, but the major heat load to the first wall comes from the particle and radiation flux. These, in turn, are strongly affected by divertors.

Neutronically, the first wall tubes and coolant may have some useful moderating, neutron multiplying, or breeding effects, but these are secondary with respect to the primary heat-transfer and plasma-wall interface functions. Thus they are not explicitly treated as useful characteristics here. However, a bound on non-useful neutron interactions is imposed by using only the relevant microscopic cross-sections in Σ_s and Σ_c

$$\exp\left[-(2\Sigma_s t + \frac{\pi}{2}\Sigma_c R)\right] \geq \Delta BR \tag{14}$$

where ΔBR is the breeding ratio reduction factor, assumed proportional to the non-useful neutron flux attenuation factor through the tubes. The $\pi R/2$ factor refers to an average

coolant thickness across the tube. The average tube thickness is, assuming thin tubes, approximated as just $2t$.

Sputtering by the particle flux limits the minimum tube thickness

$$t \geq \frac{S_i}{E_i}(q''f_p)(\tau\gamma)\left(\frac{A_s}{N_A\rho_s}\right) \tag{15}$$

where S_i is the sputtering coefficient for incident ions with energy E_i; γ is the duty factor or the fraction of total burn cycle that is actual burn; τ is the first wall life neglecting down time for maintenance; A_s is the atomic weight of the tube material; and N_A is Avogadros number. Redeposition may reduce the net sputtering rate, but it may not be uniform and is not included.

2.5 Maintenance Limits

These limits are not as strong constraints on the design as others such as temperature limits. However, it is desirable to segment the reactor toroidally into modules for ease of access and removal. For tubes running in the toroidal direction, and neglecting the possibility of multiple passes, then

$$\frac{2\pi R_m}{x} \geq N_m \tag{16}$$

where N_m is a minimum desirable number of toroidal modules and R_m is the machine major radius.

It is also desirable to limit the number of first wall tubes since reliability decreases with the complexity of the header arrangements and number of welds

$$\left(\frac{2\pi R_w}{2R}\right)\left(\frac{2\pi R_m}{x}\right) \leq N_t \tag{17}$$

where R_w is the first wall radius (the machine minor radius) and N_t is the maximum number of first wall tubes.

2.6 Design Window

A design window begins with a choice of coolant and tube material. This fixes materials properties and establishes materials-related limits. Other limits are already known from general engineering considerations. Then general reactor parameters q'', f_r, f_p, τ, R_w and R_m are chosen. Finally, tube length is fixed through the modularity constraint, Eqn.(16).

Tube thickness is bounded by fatigue life and breeding ratio from being too large, Eqns.(10) and (14); and by stress and sputtering from being too small, Eqns.(9) and (15). To be exact, the maximum tube thickness is the minimum of the fatigue life and breeding ratio bounds, while the minimum thickness is the sum of the hoop stress and sputtering thickness limits in order for the end-of-life thickness to be able to handle the coolant pressure.

From the temperature limits, Eqns.(6), (7) and (8), upper limits on ΔT_c for given R can be calculated over the range of thicknesses. Note that this requires some iteration because of the complicated way ΔT_c appears in these equations. Finally, the pumping power limit Eqn.(11), and reliability limit Eqn.(17) are plotted on $\Delta T_c - R$ axes. The result is, ideally, a region or window where all these constraints can be simultaneously satisfied.

These windows can then be used to: (1) provide a quick assessment of various blanket types and materials choices through the size and location of the design window itself; (2) provide a quick comparison of point designs by showing how close each is to the constraints for its particular geometry; (3) show which constraints are the most limiting and how sensitive the design is to them; and (4) gives the range of values for design parameters. Here we are particularly interested in how the redundancy requirement limits the design.

3.0 Materials Properties and Limits

This section describes the various constants and empirical correlations used to provide properties and limits.

3.1 Properties

Coolant property correlations were obtained from Ref.12 and Hitec data in Ref. 32. Stainless steel (316SS annealed) property correlations were included for ν_s, E_s, k_s, α_s, ρ_s, and Σ_s. The first five were obtained from the Nuclear Systems Materials Handbook [13]. Other structural material properties were obtained from Ref.[17] or the design studies that used these alloys.

Two slightly different neutron cross-sections are used to account for heating of the first wall (Σ_h) and for neutron attenuation in the first wall (Σ_{BR}).

Neutron interactions can be roughly classed into scattering or absorption. In the former, some fraction of the incident neutron energy is deposited, while in the latter, most of the energy is deposited locally. For a macroscopic heating cross-section Σ_h, and a flux ϕ_o of E_o energy neutrons, the energy absorbed per unit volume is $\phi_o E_o \Sigma_h$ ($t\Sigma_h \ll 1$) where

$$\Sigma_h = n\sigma_h = \frac{\rho_s N_A \sigma_h}{A} = \Sigma_{absorption} + \frac{\overline{\Delta E}}{E_0} \Sigma_{scattering} \qquad (18)$$

and n is the atom density. For inelastic scattering, the average energy loss is $\overline{\Delta E} \approx E_0 - 6.4(E_0/A)^{1/2}$ for a (non-magic) nucleus of mass A [14]. For elastic scattering which is isotropic in the center-of-mass system, $\overline{\Delta E} \approx E(1 - 2/3A)/(1 + A)$, except for light nuclei [15].

The neutron attenuation or breeding ratio cross-section is similarly the sum of absorption and scattering components. However, there are two main differences. First "useful" interactions such as (n,2n) or (n,T) are not included. Since the primary purpose of the first wall is to handle the surface heat load and the plasma-wall interaction, no attempt is made to optimize its breeding ability – rather a limit on the non-useful interactions is specified. The second difference is that scattering is included to the extent that it reduces the neutron energy below the 3 MeV threshold for $Li^7(n,nT)He^4$ (the Li^6 (n,T) cross-section is largest for thermal energies):

$$\Sigma_{BR} = n\sigma_{BR} = \Sigma_{\substack{non-useful \\ absorption}} + \frac{\overline{\Delta E}}{\Delta E_t} \Sigma_{scattering} \qquad (19)$$

where ΔE_t = 14 – 3 = 11 MeV if $\overline{\Delta E} < 11$ MeV, and $\Delta E_t = \overline{\Delta E}$ otherwise.

Microscopic cross-sections were obtained from Ref. [16]. Calculated cross-sections are listed in Table 1. A density-dependent macroscopic cross-section is used for coolants since moderate ranges in density are possible.

3.2 Temperature Limits

Three distinct temperature limits are considered, although the actual values may not be precise. The upper limit for corrosion is a "reasonable" temperature for long-term use in power systems. The mechanical limit corresponds to a temperature at which mechanical properties are appreciably degraded – perhaps phase transition, or simply the approach of the melting point. Even the melting point itself is not precise since it varies over the small range of compositions in any alloy specification.

Table 2 gives these temperature limits for some representative alloys, compiled from a variety of references such as Ref.[17]. The corrosion and mechanical limit temperatures are probably higher than would be used in practice, and in some cases – notably flibe/(V, Nb, Mo) and He/(V,Nb) – assume particularly pure coolant.

3.3 Stress Limits

Data for 316SS and other potential fusion reactor alloys have been analyzed according to the criteria of ASME Code Case 1592 for Class 1 Components in Elevated Temperature Service and tentative primary membrane stress limits determined [17]. For 316SS,

$$S_{mt}[10^5 \text{ hour}] = 1.08 \times 10^8 + 3.50 \times 10^{-7} T^5 - 1.22 \times 10^{-20} T^{10} \qquad (20)$$

where S_{mt} is in N/m^2, T in C and the fit is accurate to within 2% over 300 to 600 C.

The peak stress is fatigue-limited. 316SS data is obtained from a convenient fit to the ASME fatigue curves [17]

$$\log_{10}(\tau N_b) = a_1 + \frac{a_2}{a_3 + \log_{10}(\Delta\epsilon)} \qquad (21)$$

where τ is the actual operating life excluding maintenance down time in years, N_b is the number of burns/year, $\Delta\epsilon$ is the % strain range, and a_1, a_2 and a_3 are coefficients given in Ref.[17].

Pumping power is limited by plant efficiency considerations. In general, Fraas [18] recommends (pumping power)/(thermal power) < 2% for commercial power stations. Since the first wall only accepts a fraction of the total energy and considering the severe environment it operates in, a pumping power ratio (P^*) larger than 2% may be acceptable. In the present analysis, only friction pressure drop in the straight part of the first wall tubing is included while, in reality, substantial pressure drops will occur in the headers, steam generators and connecting lines. Thus the pumping power ratio in the first wall tubing itself is somewhat arbitrarily limited to 5%. However, this limit was not found to be very restrictive in the subsequent analysis.

3.4 Incident Flux Limits

Reactor breeding ratios are generally in the range 1.1 to 1.5 [3,19], allowing for parasitic absorption of the fusion neutrons in structure or coolant. In this study, an upper limit of 25% attenuation of the incident flux through non-useful interactions (i.e. excluding neutron multiplication or tritium production) in the first wall tubes and coolant is specified.

The sputtering coefficient is a function of incident particle energy, mass and direction as well as surface properties. For deuterium or tritium normally incident on iron, the sputtering coefficient is: [20,21]

$$S_i(atoms/ion) = 0.0176(E^*)^{0.25}(1 - 1/E^*)^{3.5} \tag{22}$$

where $E^* = 0.025E$ and E is the particle energy in eV. Edge energies are not well known, but will probably be in the range of 100 to 1000 eV [3,22]. In this study, 500 eV is used unless otherwise specified.

3.5 Maintenance Limits

Tokamak power reactor designs often assume relatively immobile superconducting toroidal field coils with removable blanket sections between the coils [3,23,24]. For first wall tube array designs, this limits the tube length to a fraction of the circumference (not considering serpentine paths and the associated stresses and pressure drops at the bends). The number of toroidal field coils ranges over 8 to 12 in most designs, so the minimum number of toroidal sections is about 10. However the modules can be much smaller than one-tenth of the circumference, and here we take 24 toroidal segments as representative (see Table 3).

The number of first wall tubes depends on the size of the reactor, the tube length and tube radius. Too many tubes increase the possibility of leaks at the tube/header joints. Fraas [18] estimated Mean Time Between Leaks from stainless steel experience as

$$MTBL(yr) \leq \frac{1.1 \times 10^5}{(number\ joints)}\left(\frac{50}{\Delta T_c(K)}\right)\left(\frac{E_{a,316SS}}{E_{a,tube}}\right)\left(\frac{S_{mt}t}{pR}\right) \tag{23}$$

For (number joints) $\approx 2 \times$ (number tubes), ΔT_c = 100 K, MTBL = 3 yr, 316SS tube material, S_{mt} = 100 MPa, t = 1 mm, p = 2 MPa and R = 15 mm, then $N_t < 31000$ tubes. This is clearly a rough estimate, but it is consistent with the various reactor designs listed in Table 4. In this study, we consider large power reactors also with $N_t \leq 25000$ tubes as a reasonable upper bound.

3.6 Base Reactor Parameters

While efforts have been made to make the results non-specific to particular reactor designs, quantitative conclusions require certain representative reactor parameters. Table 3 lists base reactor parameters for several reactor designs, as well as the values chosen here as representative.

Since the temperature constraints are very limiting, the choice of inlet conditions is important. Generally, for good efficiency, energy should be collected from the plasma at high coolant temperatures which favors high inlet temperature and pressure. However the larger these are, the smaller the operating margin to the temperature and stress limits. Also, since the first wall only picks up a fraction of the total reactor power, lower average temperatures are not necessarily unacceptable in terms of plant thermodynamic efficiency. In this analysis, the first wall inlet conditions of Table 4 are used. These are reasonable low-inlet temperature conditions with enough pressure to prevent boiling and provide the required driving force.

The first wall particle and radiation loading must also be specified since these are the major heat load on the first wall. The actual particle and radiation loading are affected by the divertors and limiters. From a survey of available experimental data and reactor designs, Table 5 shows the relative power distribution among first wall particle (ions and charge exchange neutrals) loading and radiation loading as a function of divertor (and/or limiter) power, expressed as fractions of the total power. Since present experiments do not produce appreciable fusion energy, these experimental results are normalized such that the sum of first wall power fraction (particles and radiation) and divertor/limiter power fraction is 20% – i.e. an effective neutron power is inferred to scale these results to power reactor conditions. While the results in Table 5 are approximate, they show a decrease in radiated power as the divertor becomes more effective and controls the impurities and that the actual particle flux to the first wall carries only a few percent of the total power. Since the actual effectiveness of divertors is still uncertain, we conservatively assume $f_d = 0.1$, and take $f_r = 0.13$ and $f_p = 0.02$ as reference parameters satisfying $f_r + f_p + f_d = 0.25$ (recall f_r, f_p and f_d are defined relative to the neutron power).

4.0 Results

Consider the main features of a representative design window (Figure 1). The acceptable operating region or design window is bounded on all sides. The maximum number of cooling tubes places a minimum tube radius limit. A maximum pumping power ratio limits the minimum coolant temperature rise – too small ΔT implies fast flow and associated high pumping power. Corrosion and mechanical temperature limits set a maximum ΔT for

given inlet conditions which is dependent on $t(R)$. Each point on the window is associated with a range of possible thicknesses, the overall window bounds are drawn based on the maximum range of thicknesses consistent with the overall constraints.

Finally, a limiting upper value for the tube radius is obtained from the operation under failure constraint. As this radius increases, the heat collected by each tube increases, as does the conduction path length for heat removal from a failed tube's hot spot to an adjacent tube. The combination of these two effects gives this limit a strong radius dependence.

4.1 Comparison of First Wall Coolants

An optimum choice for first wall material and coolant depends on safety, availability and economics, in addition to fundamental engineering design feasibility. If we neglect these other constraints except in choosing 316SS as a reasonable first wall material, we can compare the design windows for all coolants under present consideration. The comparison is made at the standard conditions discussed in Section 3, and at a wall loading of 1 MW/m^2. The pumping power ratio limit $P^* < 5\%$ is omitted for clarity because it is close to the horizontal axis.

From Figure 2, we see that all the coolants have design windows with 316SS structural material. However, there is clear preference for helium or liquid metal coolants because the higher temperature capabilities yield larger windows, which in turn allow room for conservative design and inherent fault tolerance.

Since these design limits were determined self-consistently with the "operation under failure" constraint (primarily a maximum tube radius constraint), these results indicate that leak-tolerance is possible for 316SS and all these coolants at quite reasonable tube radii – e.g. about 2.5 cm at 1 MW/m^2.

4.2 Analysis of Reference Designs

The design window methodology also allows a quick check of reference designs, which we illustrate by analyzing the Princeton tokamak design [1], HFCTR [2], NUWMAK [3], the ORNL cassette blanket [4] and FED [33]. Most base data are given in Table 3. Limits and design points are indicated in the design windows in Figure 3.

The PPPL reference tokamak design meets all constraints, falling on the design window (Figure 3a). The actual design proposed a 0.8 mm tube thickness. This just satisfies the sputtering requirement for a five year life based on their low particle flux to the first wall

(Table 5). From the design window analysis, the same overall design would work equally well if the thickness was increased to 3.7 mm. (Note lines of maximum thickness are not shown on the figures for clarity.) This would provide a margin against plasma disruptions, arcing and sputter rate uncertainties, and could allow operation under failure.

The HFCTR reference design also is within the design window (Figure 3b). However, their tube thickness was only 1.5 mm and under the design conditions of a relatively high particle flux to the first wall ($f_p = 0.17$ estimated in this analysis, see Table 5), we find 3.3 mm to be required. In this design, the tube radius is limited by the maximum thickness allowed for fatigue life and neutron attenuation equalling the minimum thickness required for the sputter rate and pressure stress loads, rather than the leak-tolerance constraint.

The ORNL cassette blanket study was a conceptual blanket design rather than a reactor design, but the blanket was analyzed in a representative reactor configuration with HITEC and helium coolants and 316SS structure. We could not obtain any design window using their deliberately conservative first wall thermal load and a pure stainless steel first wall. However, assuming more reasonable loads (2% particles, 10% divertor or limiter loads) and a coating with a ten-fold reduction in sputtering, we obtain the design windows shown in Figure 3c. The blanket study considers a range of tube radii, from 1 to 2.5 cm, but on the basis of the design window we prefer a 1 cm tube radius and 3 mm thickness.

The FED design (Ref.[33]) was not completed to the point of detailed first wall design. Nonetheless, on the basis of the known overall design parameters, we can assume a tube-array type first wall cooling system and construct the design window. The result is shown in Figure 3d, for the system described in Table 3. Thus a water-cooled 316SS tube-array first wall is a very reasonable design. The upper temperature limit is controlled by the onset of boiling, the maximum radius by the redundancy requirement, and the thickness ($t \leq 1$ cm) by neutron attenuation.

4.3 Sensitivity

A design window can be used to determine the most limiting or the most sensitive parameters. Here we will use the Li/316SS system to illustrate the effects, the other coolants behave similarly.

A major design variable is the first wall neutron power loading. In Figure 4a, increasing q'' from 0.5 to 1 MW/m^2 sharply decreases the design window. Under plausible conditions

15

of a 3 year life, less than 25% neutron attenuation, 2% particle load (as fraction of neutron load) and 500 eV incident particles, the maximum first wall load is only 1.2 MW/m^2 for 316SS, at about 8 mm tube thickness. The primary limiting feature is leak-tolerance as evidenced by the maximum allowable tube radius line on the design window of Figure 4a.

A second important variable is divertor effectiveness. The more effective the divertor, the less thermal power to the first wall. In Figure 4b, the fraction of fusion power diverted (relative to neutron power) is varied and the design window decreases as divertor effectiveness does (values of f_p and f_r were varied, but were consistent with Table 5). Again, leak-tolerance is most susceptible to this variable because decreased divertor effectiveness results in proportional increases in first wall heat loading.

With respect to the leak-tolerance design itself, calculations so far have been based on every third tube connected to the same header – i.e. a three-header first wall system. Then, if a tube fails and that header system is shut down, each remaining tube need carry only 50% more power. A two-header system, where each operating tube must carry an additional 100% power in the event of a tube failure, was not analyzed in detail. However, it requires a 30% increase in power handling capability and does not visibly affect the design window appreciably, although the required coolant velocity would be about 30% higher.

Changing the first wall life from 3 to 5 years or neutron attenuation from 25% to 10% results in no design window at all for the reference design since the minimum wall thickness exceeds the maximum thickness. On the other hand, there was little effect observed on changing the incident particle energy from 500 eV to 300 or 1000 eV, number of burn cycles from 6.3×10^4 to 6.3×10^3/year, or number of toroidal modules from 24 to 20. An alternate set of higher inlet conditions was also considered. For these, the results were essentially as shown in Figure 2, but compressed in the ΔT_c direction as expected from the higher values of T_{in}.

The fundamental parameter which controls the design window is tube thickness. Thick tubes give good conduction paths and allow operation under failure as well as good sputter life. On the other hand, the fatigue life and maximum coolant temperature rise decrease with thickness, and neutron attenuation increases. By considering the range of possible thicknesses that satisfy these constraints, we obtain the design window. Thus

16

increasing first wall loading requires more thickness to handle the increased sputtering, yet less thickness to reduce the cross-tube-wall thermal stress. Since this is satisfied by a smaller range of thicknesses, the design window decreases. Too much wall loading (or too high a particle load, too long a module life or too little neutron attenuation) cannot be satisfied by any thickness.

5.0 Conclusions

In this report we examined the tube array first wall design using a general design window methodology in which design variables are chosen in a self-consistent manner based on major engineering constraints. In particular, the possibility of operation with some failed tubes was included. The design window approach is illustrated using 316SS and Li, Na, He, Hitec, Water and Flibe coolant.

The results indicate that with these materials under plausible fusion reactor conditions are compatible with a leak-tolerant design, provided that a three-header first wall coolant system is used, and the first wall thermal load is kept below about 0.2 MW/m^2. Typically, the tube radius should be less than about 2.5 cm. This implies neutron wall loads of 1 MW/m^2, appreciably less than the 4 MW/m^2 of such recent designs as STARFIRE, but compatible with near-term demonstration machines such as FED. In any event, the principle outlined here may be compatible with higher wall loadings by adjusting other parameters – shorter tubes, for example.

The analysis also showed the preference for using liquid metals rather than flibe with 316SS, and that helium, Hitec and water were of comparable but intermediate interest. Consideration of some reference designs indicated that the design points did meet most constraints, although some sputtering rates might be optimistic. And in sensitivity analysis, we illustrated the effect of such parameters as first wall power loading and divertor effectiveness on the design.

6.0 References

1. R.G. Mills, "A Fusion Power Plant", MATT-1050, Princeton University, August 1974.

2. D. Cohn et al, "High Field Compact Tokamak Reactor (HFCTR) Conceptual Design", M.I.T., PFC/RR-78-2, March 1978.

3. B. Badger et al, "NUWMAK: A Tokamak Reactor Design Study", University of Wisconsin, UWFDM-330, March 1979.

4. R.Werner, "ORNL Fusion Power Demonstration Study: The Concept of the Cassette Blanket", ORNL/TM-5964, Oak Ridge National Laboratory, October 1977.

5. D. Aase et al, "TCT Hybrid Preconceptual Blanket Design Studies", Battelle PNL-2304, January 1978.

6. C. Stewart, M. Bramptou, D. Aase and A. Sutey, "The Limits of Helium Cooling in Fusion Reactor First Walls and Blankets", Battelle PNL-2477, January 1978.

7. M.A. Hoffman and A. Mokhtarami, "Heat Flux Limitation for Water-Cooled Extraction Grids in Ion Accelerators", ASME Paper 80-HT-50, National Heat Transfer Conference, Orlando, Florida, July 1980.

8. W. Rohsenow and H. Choi, "Heat, Mass and Momentum Transfer", Prentice-Hall, Inc., New Jersey, 1961.

9. S. Lefkowitz, "Thermal-Hydraulic Assessment of Recent Blanket Designs for Tokamak Fusion Reactors", MS thesis, M.I.T., February 1975.

10. J. Meyer, "Structural Advantages of Steady-State Fusion Power Reactors", PFC/TR-78-3, M.I.T., March 1978.

11. R. Shock, "Helium Cooling Circuits for a Fusion Reactor", Culham Laboratory, CLM-P572, February 1979.

12. P. Gierszewski, B. Mikic and N. Todreas, "Property Correlations for Lithium, Sodium, Helium, Flibe and Water in Fusion Reactor Applications", M.I.T., PFC/RR-80-12, August 1980.

13. "Nuclear Systems Materials Handbook, Vol. 1, Design Data", Hanford Engineering Development Lab, July 1980.

14. J. Lamarsh, "Nuclear Reactor Theory", Addison-Wesley Publ. Co., Reading (1972).

15. A.F. Henry, "Nuclear Reactor Analysis", M.I.T. Press, Cambridge (Massachusetts), 1975.

16. D. Garber and R. Kinsey, "Neutron Cross-sections, Vol. II, Curves", 3rd ed., BNL-325, January 1976.

17. G.P. Yu, "Relationships of Materials Properties to the Design of a Fusion Reactor First Wall", Sc.D. thesis, M.I.T., Nuclear Engineering Department, May 1981.

18. A.P. Fraas, "Comparitive Study of the More Promising Combinations of Blanket Materials, Power Conversion Systems, and Tritium Recovery and Containment Systems for Fusion Reactors, ORNL-TM-4999, November 1975.

19. J. Chao, B. Mikic and N. Todreas, "Neutronic Performance of Fusion Reactor Blankets with Different Coolants and Structural Arrangements", Nucl. Tech., 45, Sept. 1979, p. 113.

20. G.M. McCracken and P.E. Stott, "Plasma-Surface Interactions in Tokamaks", Nucl. Fusion, 19 (7), July 1979, p. 889.

21. M. Gardinier, "The Impact of Plasma Wall Interactions on the Burn Dynamics of Tokamak Reactors", UWFDM-356, May 1980.

22. S.A. Cohen, "The Flux of Hydrogen from Tokamak Devices", Session XI, Transactions of the Fourth Topical Meeting, The Technology of Controlled Nuclear Fusion, October 14-17, 1980, King of Prussia, Pennsylvania, p. 315.

23. D. Steiner and P.H. Rutherford, "ETF Interim Design Review", Presentations at Opening Plenary Session, Rockville, Maryland, July 23, 1980, U.S.D.O.E.

24. C.C. Baker et al, "STARFIRE – A Commercial Tokamak Fusion Power Plant Study", ANL/FPP-80-1, Argonne National Laboratory, September 1980.

25. B. Badger et al, "UWMAK-III, A Noncircular Tokamak Power Reactor Design", Vol. I, EPRI ER-368, July 1976.

26. B.Badger et al, "UWMAK-I", University of Wisconsin, UWFDM-68, March 1974.

27. B.Badger et al, "UWMAK-II – A Conceptual Tokamak Reactor Design", University of Wisconsin, UWFDM-112, October 1975.

28. ASDEX Team, "Divertor Experiments in ASDEX", IPP Garching III/173, October 1981.

29. R.L.Haueter et al, "Equipment Availability Component Cause Code Summary Report for the Ten-Year Period, 1967-1976", EEI Publ. No. 77-64A, Edison Electric Institute, New York, January 1978.

30. DIVA Group, "Divertor Experiment in DIVA", Nucl. Fus., 18(12), 1978, 1619.

31. L.Scaturro and M.Pickrell, "Bolometric Measurements and the Role of Radiation in Alcator-A Power Balance", PFC/RR-79-8, M.I.T., 1979.

32. D.L. Smith et al, "Fusion Reactor Blanket/Shield Design Study", ANL/FPP-79-1, July 1979.

33. C.A.Flanagan et al, "Initial Trade and Design Studies for the Fusion Engineering Device", ORNL/TM-7777, Oak Ridge National Laboratory, June 1981.

34. E.Schuster et al, "Escape of Fission Products from Defective Fuel Rods of Light Water Reactors", Nucl. Eng. and Design, 64, 81 (1981).

35. M.A.Hoffman, "Heat Flux Capabilities of first-Wall Tube Arrays for an Experimental Fusion Reactor", Nucl. Eng. and Design, 64, 283 (1981).

36. J.Chao, P.Gierszewski, B.B.Mikic and N.E.Todreas, "A Performance Comparison of Lithium, Helium and Flibe Cooled Tube/Header Fusion Blankets", Journal of Fusion Energy, 2(2), April 1982.

Table 1: Macroscopic Cross-sections

Material	Assumed Composition (atom %)	ρ^2 (Mg/m^3)	M_w (g/g-mole)	σ_h^1 (b)	σ_{BR}^1 (b)	Σ_h (1/m)	Σ_{BR} (1/m)
316SS	100 Fe	7.98	56	1.30	1.65	11.2	14.2
Nb-1Zr	100 Nb	8.6	93	1.36	1.54	7.4	8.6
TZM	100 Mo	10.2	96	1.86	2.15	11.9	13.8
V-20Ti	100 V	6.1	51	10.50	0.69	3.6	5.0
Inconel-718	100 Ni	8.9	59	1.00	1.22	9.1	11.1
Al	100 Al	2.7	27	0.77	0.93	4.6	5.6
Lithium	100 Li	0.47	7	0.24	0.19	0.95	0.77
Sodium	100 Na	0.80	23	0.54	0.85	1.13	1.78
Helium	100 He	0.0054	4	0.16	0.21	0.013	0.017
Flibe	60 F/20 Li/20 Be	1.95	73	0.39	0.48	0.63	0.77
Hitec	12 Na/22 N/56 O/10 K	1.65	84	0.43	0.53	0.51	0.63
Water	33 O/67 H	0.70	18	0.24	0.28	0.56	0.66

Notes:

1: $1 \text{ b} = 1 \text{ barn} = 10^{-28} \text{ m}^2$

2: Representative values. Coolant evaluated at:

Li 0.3 Mpa 600 C; Na 0.3 MPa 600 C; He 10. MPa 600 C;

Flibe 0.3 MPa 600 C; Hitec 0.3 MPa 600 C; Water 10. MPa 300 C.

Table 2:   Temperature Limits

Alloy	Corrosion Temperature Limit						Mechanical Properties Limit	Melting Point
	Li	Na	He	Flibe	Hitec	Water		
316SS	500	700	750	650	500	550	550	1430
Nb-1Zr	1000	1200	500	650	—	—	800	2470
TZM	1000	1000	850	1000	—	—	950	2610
V-20Ti	800	500	450	700	—	—	700	1900
Inconel-625	500	800	830	500	280	—	600	1450
PE-16		700					700	1330

Table 3: Reactor Parameters

Study	PPPL	UWMAK-III	ORNL	HFCTR	NUWMAK	STARFIRE	ETF	FED	This[3]
Structure	PE-16	TZM	316SS	TZM	Ti	316SS	316SS	316SS	316SS
Coolant	He	He/Li	He/Hitec	Flibe	Water	Water	Water	Water	-
R_m(m)	11.	8.1	6.0	6.0	5.1	7.0	5.4	6.0	6.0
R_w(m)[1]	3.6	2.7	1.5	1.2	1.4	2.8	1.4	1.5	1.5
τ(yr)	5	30	2	4	4	6	-	10	3
N_b(burns/y)	5250	18000	63000	55000	130000	1	230000	31450	63000
γ(%)	97.	95.	90.	87.	91.	100.	74.	10.	90.
N_t	24730	1170	6280	7040	4960	23000	-	-	25000
N_m	24	18	9[2]	8	8	24	15	10	24
p_{in}(MPa)	5.	7./	6./0.7	1.	8.6	15.2	-	0.69	-
T_{in}(C)	95	488/	77/142	544	300	320	-	60	-
P^*(%)	5	-	2	0.5	5	-	-	-	5
ΔBR	0.9	-	0.9	0.9	0.9	-	-	-	0.75
q''(MW/m^2)	1.65	2.5	3	4.0	4.0	3.6	1.5	0.8	1
f_p	0.002	0.013	-	0.17	0.04	-	0.016	0.	0.02
f_r	0.20	0.002	-	0.08	0.04	0.25	0.024	0.19	0.13
E_i(eV)	300	-	-	300	324	1200	300	300	500
R(cm)	1.2	2.0/	1.	0.6	1.2	0.2	-	-	-
t(mm)	0.08	1./	-	1.5	1.5	1.5	-	12.5	-
ΔT_c(C)	355	382/	250/185	36	0	40	-	40	-
Report	[1]	[25]	[4]	[2]	[3]	[24]	[23]	[33]	-

Notes:

1: Aspect ratio effects not necessarily accounted for.

2: First wall tubes run poloidally. N_m = (on-axis circumference)/(actual tube length).

3: Reference or representative parameters used in this report in generic analyses, or when design studies did not specify values.

Table 4: Reference Inlet Conditions

Coolant	p_{in} (MPa)	T_{in} (C)	T_{melt} (C) (0.1 MPa)	T_{boil} (C) (0.1 MPa)
Lithium	0.5	250	180	1340
Sodium	0.5.	150	98	880
Helium	6.0	250	–	–
Flibe	0.5	400	360[1]	1430
Hitec	0.5	200	142	–
Water	10.	150	0	100

Note:

1: Eutectic flibe (47 mole %LiF).

Table 5: Fusion Power Distribution

Reference	Divertor (%)	Limiters (%)	Ions (%)	CX Neutrals (%)	Radiation (%)	Neutrons (%)
UWMAK-I [26]	5.4	0.		——0.6——	13.9	80.
	1.0	0.	0.1————		18.8	80.
UWMAK-II [27]	16.6	0.	——— 2.6 ———			81.
UWMAK-III [25]	18.	0.	——0.2——		1.6	80.
NUWMAK [3]	0.	13.8	——2.9——		3.3	80.[3]
	0.	11.0	——1.3——		7.8	80.[3]
PPPL [1]	3.9	0.	——0.02——		16.	80.
HFCTR [2]	0.	———17.3———			5.9	76.8[2]
STARFIRE [24]		3.5			19.5	77.[2]
ETF 1 [23]	13.5	0.	0.8	1.6	4.3	79.7
ETF 2 [23]	13.5	0.	0	1.6	5.1	79.7
DIVA [30]	0	—12.9———		0.6	6.5	(80)[1]
	10.7	—3.6———		1.4	4.3	(80)[1]
ALCATOR-A [31]		12			8	(80)[1]
ASDEX [28]	0	?		9.2		(80)[1]
	13.6	0		3.0		(80)[1]

Notes:

1: Power distribution fractions normalized to 20% , to be comparable with power reactor figures.

2: HFCTR includes 100 MW neutral beams, STARFIRE includes 120 MW RF power.

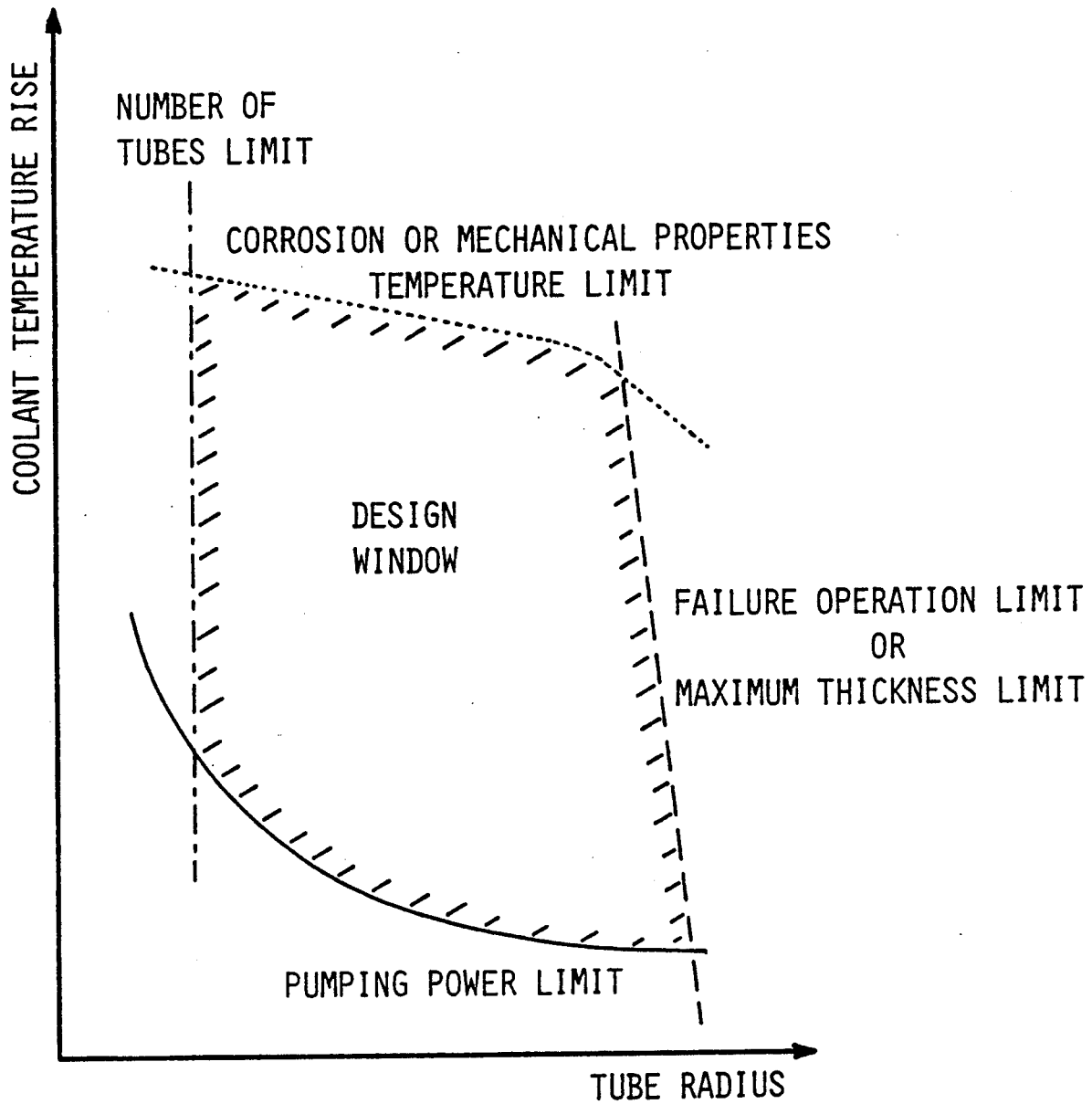3: Pure gas puffing; gas and pellet fuelling – reference cases.

FIGURE 1: REPRESENTATIVE DESIGN WINDOW SHOWING
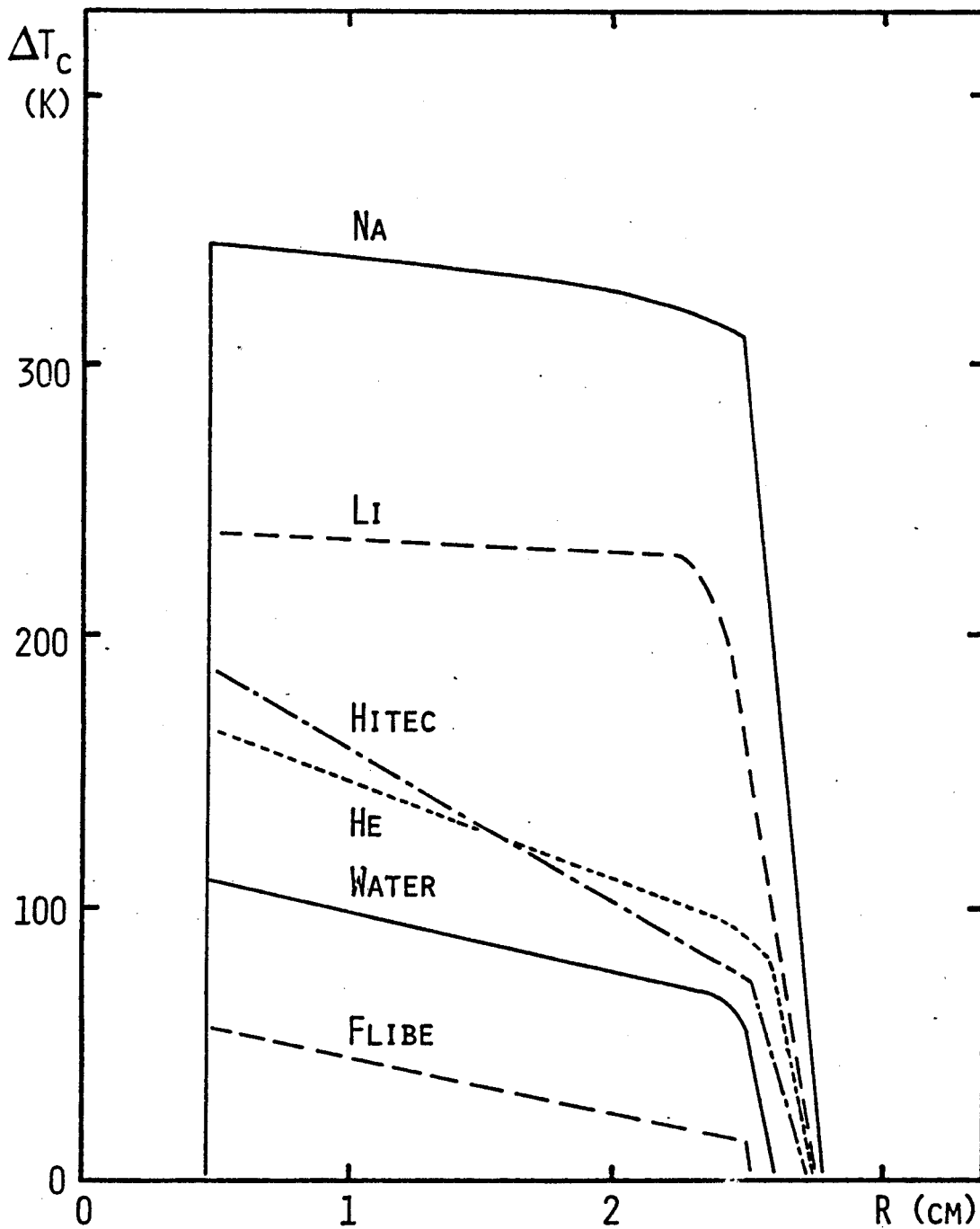KEY LIMITING PARAMETERS.

FIGURE 2: DESIGN WINDOWS FOR DIFFERENT COOLANTS WITH
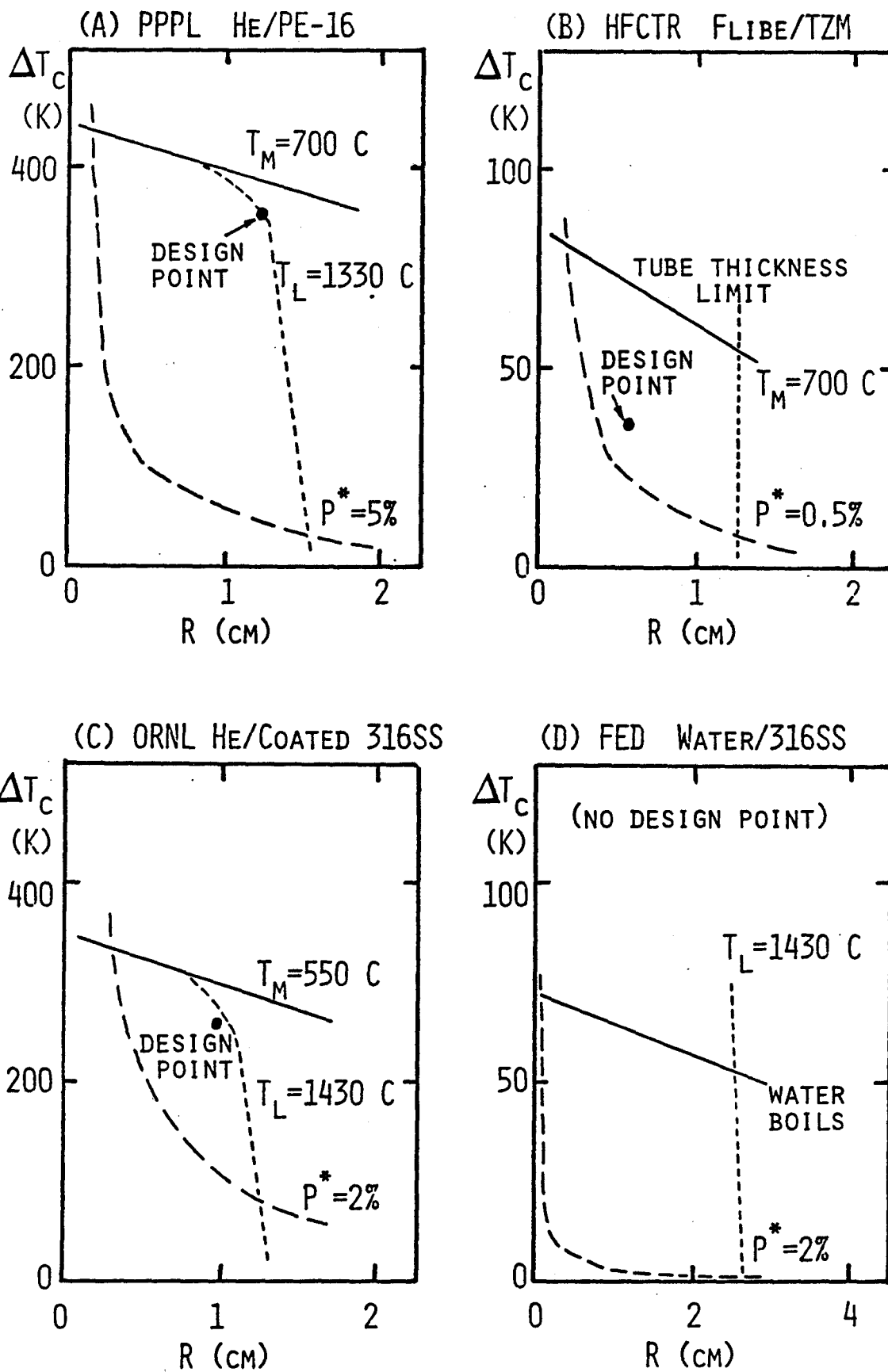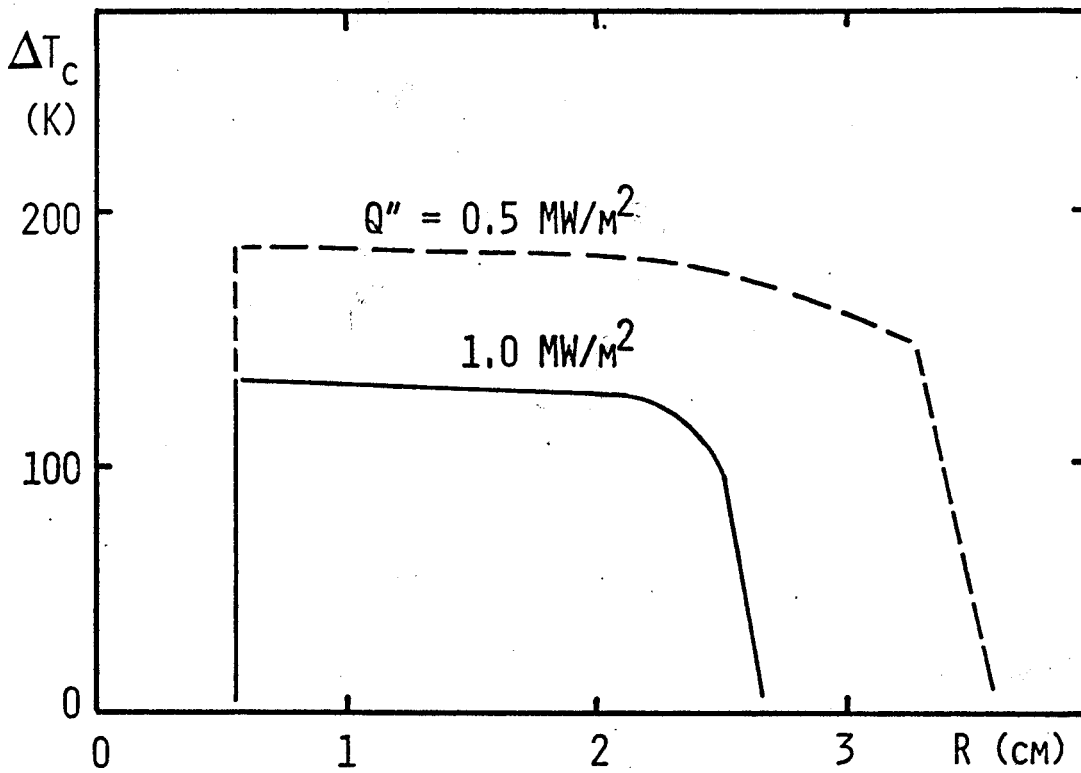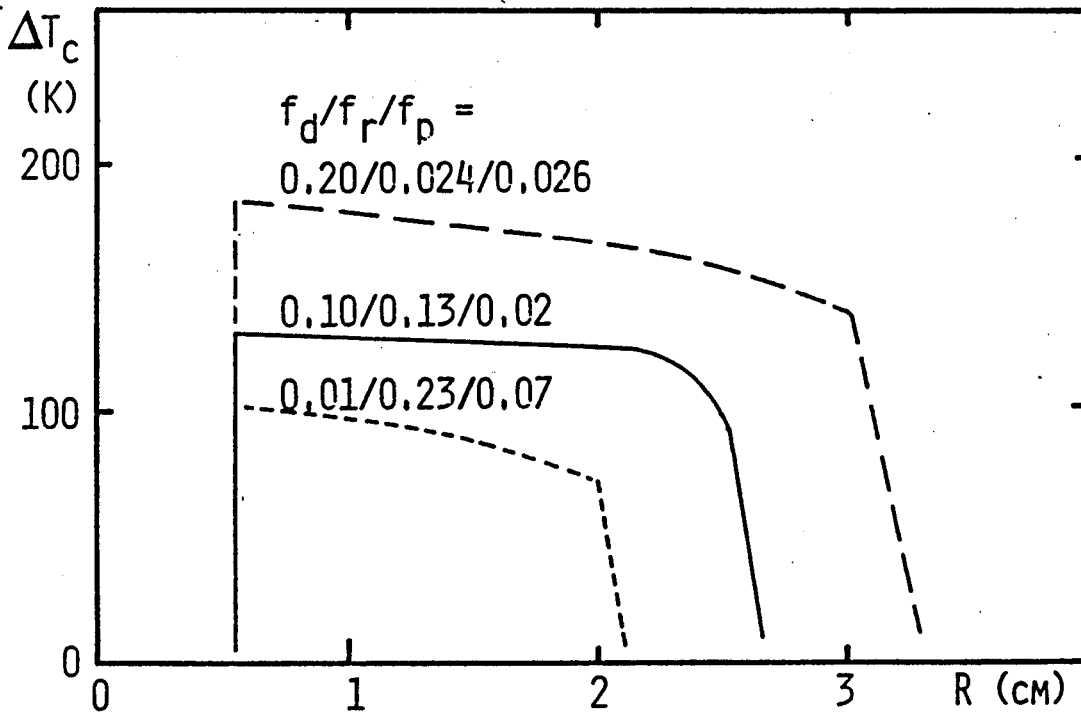316SS STRUCTURE AND REFERENCE REACTOR CONDITIONS.

FIGURE 3: ANALYSIS OF FOUR REACTOR DESIGNS. INTERIOR OF LIMIT LINES IS ACCEPTABLE OPERATING REGION.

28

(A) VARYING FIRST WALL LOAD

(B) VARYING DIVERTOR EFFECTIVENESS

FIGURE 4: SENSITIVITY OF L$_I$/316SS DESIGN WINDOW.